Tracing metal–silicate segregation and late veneer in the Earth and the ureilite parent body with palladium stable isotopes

Creech, J. B.; Moynier, F.; Bizzarro, Martin

Published in:
Geochimica et Cosmochimica Acta

DOI:
10.1016/j.gca.2017.04.040

Publication date:
2017

Document version
Publisher's PDF, also known as Version of record

Available online at www.sciencedirect.com

ScienceDirect

Geochimica et Cosmochimica Acta 216 (2017) 28–41

Geochimica et Cosmochimica Acta

www.elsevier.com/locate/gca

Tracing metal–silicate segregation and late veneer in the Earth and the ureilite parent body with palladium stable isotopes

J.B. Creech [a,*], F. Moynier [a,b], M. Bizzarro [c]

[a] Institut de Physique du Globe de Paris, Université Sorbonne Paris Cité, Université Paris Diderot, 1 Rue Jussieu, 75328 Paris cedex 05, France
[b] Institut Universitaire de France, 75005 Paris, France
[c] Centre for Star and Planet Formation, Natural History Museum of Denmark, University of Copenhagen, Øster Voldgade 5-7, DK-1350 Copenhagen, Denmark

Received 2 December 2016; accepted in revised form 28 April 2017; available online 8 May 2017

Abstract

Stable isotope studies of highly siderophile elements (HSE) have the potential to yield valuable insights into a range of geological processes. In particular, the strong partitioning of these elements into metal over silicates may lead to stable isotope fractionation during metal–silicate segregation, making them sensitive tracers of planetary differentiation processes. We present the first techniques for the precise determination of palladium stable isotopes by MC-ICPMS using a ^{106}Pd–^{110}Pd double-spike to correct for instrumental mass fractionation. Results are expressed as the per mil (‰) difference in the ^{106}Pd/^{105}Pd ratio (δ^{106}Pd) relative to an in-house solution standard (Pd_IPGP) in the absence of a certified Pd isotopic standard. Repeated analyses of the Pd isotopic composition of the chondrite Allende demonstrate the external reproducibility of the technique of ±0.032‰ on δ^{106}Pd. Using these techniques, we have analysed Pd stable isotopes from a range of terrestrial and extraterrestrial samples. We find that chondrites define a mean $\delta^{106}Pd_{chondrite} = -0.19 \pm 0.05$‰. Ureilites reveal a weak trend towards heavier δ^{106}Pd with decreasing Pd content, similar to recent findings based on Pt stable isotopes (Creech et al., 2017), although fractionation of Pd isotopes is significantly less than for Pt, possibly related to its weaker metal–silicate partitioning behaviour and the limited field shift effect. Terrestrial mantle samples have a mean $\delta^{106}Pd_{mantle} = -0.182 \pm 0.130$‰, which is consistent with a late-veneer of chondritic material after core formation.

Keywords: Palladium; Stable isotopes; Terrestrial planet accretion; Late-veneer; Meteorites

1. INTRODUCTION

The platinum group elements (PGE; Rh, Ru, Pd, Os, Ir and Pt) all exhibit highly siderophile behaviour, with the bulk of Earth's highly siderophile element (HSE; i.e., PGE + Re, Au) budget concentrated into the core. As such, the HSE have played a key role in constraining models of Earth's accretion and differentiation. Combined with their extreme depletion in the bulk silicate Earth, changes in oxidation state and bonding environment between mantle silicates and the Fe–Ni metallic core may lead to significant fractionation in HSE stable isotopes in the silicate mantles of terrestrial planets. This has led to considerable interest in stable isotope measurements of HSE, and stable isotope data for various sample types have recently been documented for Pt (Creech et al., 2014, 2017), Ru (Hopp et al., 2016) and Os (Nanne et al., 2017). Palladium represents a natural addition to this suite of stable isotope tracers, with potential to complement and contrast with these other HSE stable isotope systems.

Palladium is a transition metal with six naturally occurring stable isotopes—^{102}Pd, ^{104}Pd, ^{105}Pd, ^{106}Pd, ^{108}Pd,

* Corresponding author.
E-mail address: creech@ipgp.fr (J.B. Creech).

http://dx.doi.org/10.1016/j.gca.2017.04.040
0016-7037/

^{110}Pd—with relative abundances of 1.02%, 11.14%, 22.33%, 27.33%, 26.46% and 11.72%, respectively (Meija et al., 2016; Fig. 1). Palladium can occur in a number of oxidation states, although principally occurs in nature as Pd(0) and Pd(II) (Dennen, 1954; Borisov et al., 1994). Palladium shares the highly siderophile nature of the PGEs, as evidenced by its relative depletion in the mantle as compared with chondritic meteorites (chondrites: ~1 μg g^{-1} Pd; bulk silicate Earth: 4 ng g^{-1} Pd; McDonough, 2014). However, reported metal–silicate partition coefficients for Pd at conditions relevant to core formation are around an order of magnitude lower than those for the other PGE, including Pt ($D_{Pd}^{met/sil} \sim 10^3$–$10^4$; $D_{Pt}^{met/sil} \sim 10^4$–$10^5$; Holzheid et al., 2000; Mann et al., 2012). The PGE also exhibit chalcophile behaviour and in the conditions found in the mantle and crust they are most commonly found in sulphide components of ultramafic complexes. In addition to its weaker metal–silicate partitioning, Pd has the lowest density (11,995 kg m^{-3}; Kaye and Laby, 1995), melting point (1555 °C; Kaye and Laby, 1995), and 50% condensation temperature (1324 K; Lodders, 2003) of the PGE. Previous isotopic studies of Pd have been limited to searches for cosmogenic and nucleosynthetic effects in iron meteorites (Mayer et al., 2015), and as part of an experimental and theoretical study of nuclear volume effects Fujii et al. (2011). However, stable isotope variations of Pd in nature remain unexplored. The properties of Pd, in particular the relatively low condensation temperature, combined with subtle differences in the geochemistry of Pd as compared with Pt, its closest associate amongst the PGE, could lead to differences in stable isotopic compositions in nature.

Stable isotopic fractionations at temperatures relevant to metal–silicate differentiation have now been reported in several stable isotope systems, (e.g., Si (e.g., Young et al., 2015), Mo (Hin et al., 2013; Burkhardt et al., 2014), Zn (Mahan et al., 2017) and Fe (Elardo and Shahar, 2017)). The metal–silicate partitioning of Pd is significantly greater than for these elements, and combined with the differences in oxidation state and bonding environment between mantle silicates and the Fe–Ni metallic core, as well as evidence for Pt stable isotope fractionation related to metal–silicate partitioning (Creech et al., 2017), significant Pd stable isotopic fractionation could occur during planetary core formation. Stable isotopic studies of Pd, especially where contrasted with similar data for Pt, may provide useful insights into a variety of planetary and geological processes.

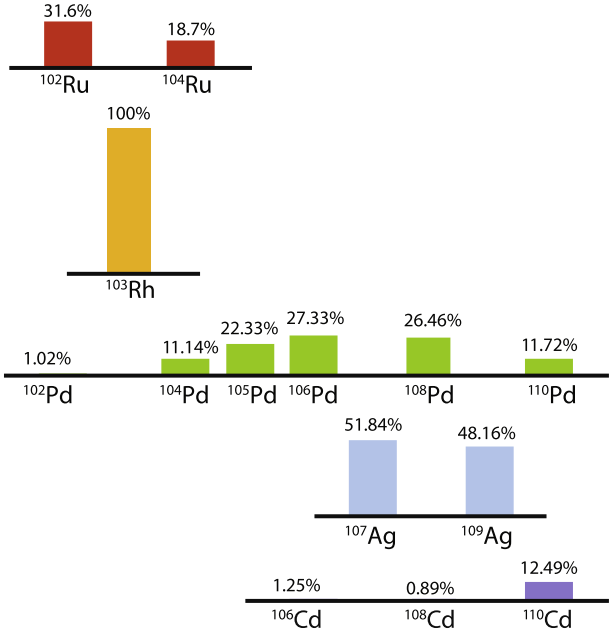

Fig. 1. Relative abundances of isotopes in the mass range of Pd from Meija et al. (2016).

In this paper, we present the first high-precision method to analyse the stable isotopic composition of Pd. We apply this technique to estimate the Pd isotopic composition of a wide range of chondrites and some modern terrestrial samples in order to provide a reference for the Pd isotopic composition of Solar System materials. We compare this solar system Pd isotopic composition to terrestrial Archean samples from Isua and South Africa to investigate the potential preservation of Pd isotopic signatures from prior to the late arrival of chondritic material, similar to those recently observed for Pt (Creech et al., 2017). We further analysed the Pd isotopic composition of a series of ureilite meteorites. Ureilites have a complex petrogenesis, but are considered to be mantle restites formed on a parent body that never totally melted (e.g., Scott et al., 1993; Barrat et al., 2015; Greenwood et al., 2016). The ureilites have HSE contents ranging from approximately chondritic to depletions of several orders of magnitude relative to chondrites (Warren et al., 2006; Rankenburg et al., 2008), which have been interpreted to reflect the early stages of core formation (Warren et al., 2006). These depletions have also been recently shown to have correlated stable isotope fractionations for the element Pt (Creech et al., 2017). These factors, combined with ureilites being among the most common achondrites in our meteorite collections (~400 ureilites are currently reported in the Meteoritical Bulletin Database) make these meteorites some of the best available samples to test the effects of metal–silicate or metal–sulphide segregation on the Pd isotopic composition.

2. DESIGN AND PREPARATION OF THE PALLADIUM DOUBLE-SPIKE

The double-spike method is a well established approach for precise determination of isotope ratios, and has been applied to a broad range of isotope systems using both TIMS and MC-ICPMS analysis (e.g., Pb, Cr, Zn, Fe, Ni, Ti, Mo, Ca, Pt, W; Compston and Oversby, 1969; Eugster et al., 1969; Hamelin et al., 1985; Beard et al., 1999; Beard and Johnson, 1999; Anbar et al., 2001; Siebert et al., 2001; Baker et al., 2004; Dideriksen et al., 2006; Gopalan et al., 2006; Schoenberg et al., 2008; Arnold et al., 2010; Gall et al., 2012; Creech et al., 2013; Hin et al., 2013; Burkhardt et al., 2014; Abraham et al., 2015; Bonnand et al., 2016; Millet et al., 2016; Bezard et al., 2016; Krabbe et al., 2017). These include several recent applications to studying mass-dependent fractionation of PGEs (Creech et al., 2014, 2017; Hopp et al.,

2016; Nanne et al., 2017). An advantage of the double-spike approach is that, where mass-dependent isotopic fractionation is being studied, the natural isotopic fractionation can be determined from a single isotope measurement, and the double-spike can correct for any mass-dependent isotope fractionation induced during chemical purification and mass spectrometry. Therefore, the double-spike method is less susceptible to potential analytical artefacts induced by trace amounts of sample matrix that may remain and incomplete yields of the analyte following chemical purification. In addition, the double-spike also permits for precise and accurate determination of Pd concentrations from the same analysis as the isotope data.

2.1. Palladium double-spike design

With six stable isotopes, there are many different possible combinations available for the Pd double-spike and the double-spike inversion. The choice of Pd double-spike was made on the basis of minimum predicted errors as calculated using the *Double Spike Toolbox* of Rudge et al. (2009), with the additional constraint that the isotopes used in the double-spike and the double-spike inversion not contain ^{102}Pd or ^{104}Pd due to the potential for interference on those isotopes from small amounts of ^{102}Ru and ^{104}Ru (Fig. 1). We therefore chose to use a ^{106}Pd–^{110}Pd double-spike using a ^{105}Pd–^{106}Pd–^{108}Pd–^{110}Pd inversion, as this combination has a small predicted error (ca. 29 ppm/amu; Rudge et al., 2009) and a broad plateau in predicted error across a range of sample–spike mixtures (Fig. 2A), indicating that this combination is not highly sensitive to the sample–spike ratio.

2.2. Preparation of Pd double-spike

Two Pd isotope spikes (^{106}Pd, ^{110}Pd) were obtained from Isoflex (www.isoflex.com) in the form of metal powders, with certified isotopic compositions as given in Table 1. The spikes were carefully weighed before transferring to Savillex Teflon beakers for dissolution with aqua regia. Once the spike material was fully digested, the spike solutions were repeatedly evaporated to dryness in concentrated HCl, and finally redissolved in 6 M HCl.

The ^{106}Pd–^{110}Pd double-spike was prepared by mixing the two spikes in the optimal proportions of (47.17% ^{106}Pd, 52.83% ^{110}Pd as calculated using the *Double Spike Toolbox* of Rudge et al. (2009). The double-spike mixture was then evaporated to dryness, taken up in a small volume of concentrated HCl, evaporated to dryness again, and finally taken up in 6 M HCl. Precise isotopic determination by the double-spike technique requires accurate calibration of the double-spike composition. The method for calibration of the double-spike prepared here and the accuracy of the calibrations are described below.

3. MATERIALS AND METHODS

3.1. Chemicals and standard solutions

All laboratory work was performed in a class-100 clean room environment using class-10 laminar flow hoods at the Institut de Physique du Globe de Paris, France. Pre-cleaned Savillex Teflon PFA beakers were used for all samples and solutions processed in this study. BASF Selectipur® AR grade acids (69% HNO_3, 37% HCl) were further purified by sub-boiling distillation using Savillex DST-1000. All dilutions were carried out using ultra-pure (18.2 MΩ cm) Milli-Q water.

Due to the unavailability of any certified isotope reference materials for Pd, we employed a Pd ICP solution standard for this purpose (Fischer Chemical 1000 mg L^{-1} Pd in 5% HCl, lot #C64130). This solution standard is hereafter referred to as Pd_IPGP; aliquots of Pd_IPGP standard can be made available to other laboratories on request.

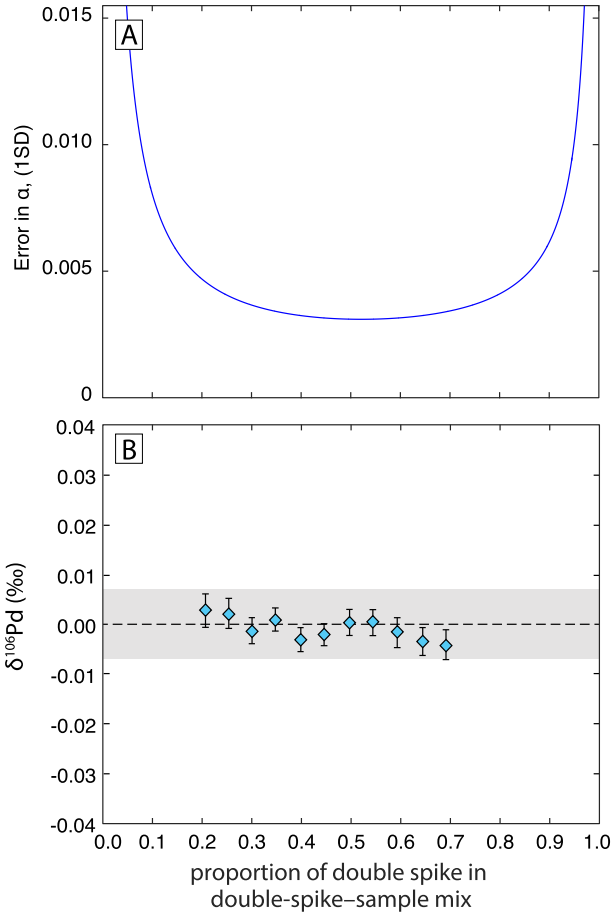

Fig. 2. (A) for the ^{106}Pd–^{110}Pd double-spike with ^{105}Pd–^{106}Pd–^{108}Pd–^{110}Pd inversion, as a function of double-spike–sample proportions, calculated using the *Double Spike Toolbox* of Rudge et al. (2009). Note that this combination results in a relatively broad region around the optimum where low errors are found. (B) Measured δ^{106}Pd as a function of the proportion of double-spike in the double-spike–sample mixture from 0.2 to 0.7, equivalent to a standard–spike ratio from 4.0 to 0.4, or a factor of 0.38–1.3 times the theoretical optimal spike–sample proportion of 0.525. Double-spike corrected results yield delta values (δ^{106}Pd) that are within the typical reproducibility of measurements of the standard over this range of sample-spike mixtures. Error bars represent the 2 s.e. on individual measurements.

Table 1
Certified isotopic compositions of single isotope spikes provided by Isoflex, and calibrated composition of ^{106}Pd–^{110}Pd double-spike.

Spike	Form	Certificate No.	^{102}Pd (%)	^{104}Pd (%)	^{105}Pd (%)	^{106}Pd (%)	^{108}Pd (%)	^{110}Pd
Pd-106	metal powder	6106	<0.03	0.06	0.68	98.4	0.80	0.6
Pd-110	metal powder	6107	<0.01	0.05	0.09	0.13	0.33	99.4
^{106}Pd–^{110}Pd double-spike			0.002	0.052	0.396	48.110	0.557	50.882

3.2. Terrestrial and meteorite samples

Details of the samples and amounts used in this study are summarised in Table 4.

Eight terrestrial samples were studied. OKUM is an ultramafic komatiite (previously distributed by Geosciences Laboratories, now distributed by IAG) sampled from Serpentine Mountain, Ontario, Canada. This area is located at the western end of the Abitibi Greenstone Belt, and was emplaced into the crust ca. 2.7 Ga (Houlé et al., 2009). PGE in these rocks are found as Ni–Cu–PGE minerals (Houlé et al., 2009). B25 is a komatiite from the ca. 3.5 Ga Barberton greenstone belt, South Africa (Caro et al., 2006). BC7 is a peridotite xenolith from Batchelor's Crater, a Plio–Pleistocene alkali basalt vent in the Chudleigh volcanic province, North Queensland, Australia. LK-NIP is a dolerite from the Nipigon Diabase, Ontario, Canada distributed by Geosciences Laboratories. The Nipigon diabase sills were intruded into the crust ca. 1100 Ma (Hart and MacDonald, 2007; Heaman et al., 2007). Four metabasalts from the Isua Supracrustal Belt were analysed from Pd cuts that were kept from previous Pt chemistry by Creech et al. (2017). In the southwest part of the belt, pillow lava structures are recognised within low deformation zone windows within a sequence of amphibolite rocks. Compositionally, the pillows are high-MgO (12–15 wt.%) tholeiitic basalts and are associated with ultramafic schists of komatiitic composition. A felsic unit which cross-cuts this pillow lava-bearing sequence gives U-Pb SHRIMP ages clustering around ~3.85 Ga (Michard-Vitrac et al., 1977; Baadsgaard et al., 1984; Nutman et al., 1997) suggesting that these amphibolites are amongst the oldest of the Isua supracrustals.

The Pd isotopic composition of 11 chondritic meteorites were analysed in this study. These comprise six carbonaceous chondrites, four ordinary chondrites and one enstatite chondrite. For one carbonaceous chondrite (Allende), a large specimen of ca. 15 g was crushed and homogenised with an agate mortar and pestle, and from this homogenised powder seven replicate digestions of ~0.7–1.0 g each were prepared. Ten Antarctic ureilite meteorites were analysed from a suite provided by NASA-JSC. These specimens span a large compositional range, with Pd contents ranging from ca. 21–165 ng/g (Rankenburg et al., 2008; Table 4), and have also been analysed for Pt stable isotopes by Creech et al. (2017).

3.3. Sample preparation and dissolution

Digestions of meteorite and terrestrial samples were carried out using a NiS fire assay method as described by Creech et al. (2014, 2017). Terrestrial samples were coarsely crushed and then powdered using an agate ball mill. Powders were weighed directly into porcelain crucibles for NiS digestion. Meteorite fragments were taken from sliced specimens, weighed and then cleaned by rinsing in ultra-pure water, methanol and again in ultra-pure water. The meteorite fragments, typically weighing 0.5–1.0 g, were then placed in a Savillex Teflon beaker in ca. 4 mL of 2 M HCl. The beakers were heated to 120 °C for ca. 10 min and then ultrasonicated for ca. 3 min. After this gentle acid washing, the samples were rinsed twice with water and then dried in the beaker on a hotplate. The samples were then crushed to a fine powder in an agate mortar and weighed before being transferred to porcelain crucibles for NiS fire assay digestion. NiS fire assays were carried out as described by Creech et al. (2014), with 10 g of sodium carbonate, 20 g of sodium tetraborate, 1 g of nickel powder and 0.75 g of sulphur being added per 15 g of sample. Note that where less than 15 g of sample was processed, the amount of sample was made up to 15 g with pure silica.

Samples were double-spiked prior to NiS digestion by adding the spike directly to the mixture in the crucible and allowing to dry before being fused in a furnace at ca. 1030 °C for 90 min. Samples were optimally spiked in approximate proportions of 52.5% Pd from the double-spike and 47.5% from the sample. Where published Pd concentrations were unavailable they were estimated based on published results for similar samples. NiS beads were extracted from fused charges and dissolved in concentrated HCl as described by Creech et al. (2014). Once fully digested, the samples were brought into solution in 10 mL of 0.5 M HCl for anion-exchange chemistry.

3.4. Chemical separation of Pd

A protocol for the chemical separation of Pt from geological materials was presented by Creech et al. (2014), utilising AG1-X8 (100–200 mesh) anion exchange resin (Table 2). In that method, the major cationic species in geological samples are readily removed from the column using dilute acids, and the PGE are eluted using sequentially stronger HCl and HNO_3. In order that in the future Pt and Pd isotopic composition may be analysed from the same samples, we employed this same method for Pd.

In this method, 1 mL of pre-cleaned AG1-X8 (100–200 mesh, chloride form) was loaded as a slurry onto Eichrom polypropylene columns with a 2 mL resin capacity and a 20 mL reservoir, and allowed to gravity settle. The resin bed was cleaned with 20 mL of 0.8 M HNO_3, 10 mL of 11 M HCl, 25 mL of 13.5 M HNO_3 and 40 mL of 6 M HCl, and then conditioned with 40 mL of 0.5 M HCl prior

Table 2
Elution scheme for Pd based on Creech et al. (2014).

Step	Eluent	Volume (mL)
Load 1 ml AG1-X8 100–200 #		
Clean column	0.5 M HNO_3	20
Clean column	11 M HCl	10
Clean column	13.5 M HNO_3	25
Clean column	6 M HCl	40
Conditioning	0.5 M HCl	40
Sample load	0.5 M HCl	10
Rinse (elute matrix)	0.5 M HCl	40
Rinse	1 M HCl	20
Discard transition metals	0.8 M HNO_3	20
Collect Pd (+Re, Ru)	11 M HCl	60
Collect Pt	13.5 M HNO_3	40

to sample loading. Samples were loaded onto the columns in 10 mL of 0.5 M HCl, which was followed by a rinse with 40 mL of 0.5 M HCl, during which virtually all of the major cationic constituents of the sample and some of the weakly retained PGE (Rh, Ru and Ir) were eluted. This was followed by elution of 20 mL of 1 M HCl to elute any remaining weakly retained PGE, and 20 mL of 0.8 M HNO_3 to elute any remaining transition metals such as Zn. The remaining PGE are recovered from the column in 11 M HCl (Ru, Pd, Re) and 13.5 M HNO_3 (Pt).

Palladium is eluted from the column in 11 M HCl with recovery of ca. 96%. However, Ru and Re are also eluted in the same cut, with yields of ca. 37% and 94%, respectively (Fig. 3). Given that (1) there are no isobaric or likely polyatomic interferences arising from the presence of small amounts of Re, (2) that while Ru has isotopes at masses 102 and 104, these isobars of ^{102}Pd and ^{104}Pd can be avoided in the double-spike inversion, and (3) the double-spike approach has been shown to be less sensitive to the presence of minor amounts of remaining matrix elements

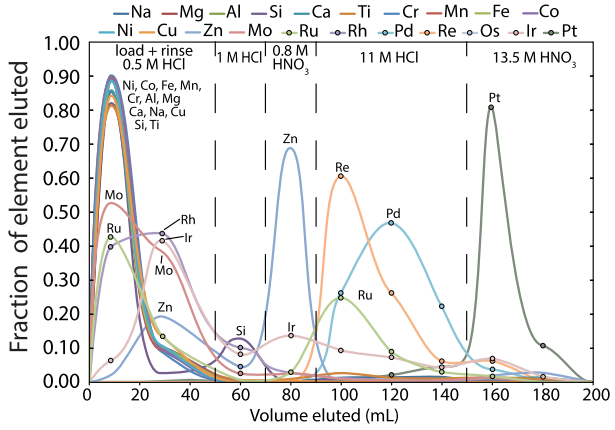

Fig. 3. Elution profile for a synthetic matrix with a chondritic composition. Major cationic components are not retained on the column and are eluted with the load and 0.5 M HCl rinse. The PGE are eluted in a sequence of HCl and HNO_3 acids. Pd is eluted in 11 M HCl with recovery of ca. 96%, although the Pd cut also contains some Ru and Re.

than sample–standard bracketing methods (e.g., Dideriksen et al., 2006; Creech et al., 2014), we trialled making measurements on Pd cuts without further purification. A range of doping tests were conducted to test the suitability of this approach for analysis of natural samples, and these are presented in Section 4.2 below.

3.5. Mass spectrometry and data reduction

Palladium stable isotope measurements were carried out using a Thermo-Scientific Neptune Plus multi-collector inductively-coupled-plasma mass-spectrometer (MC-ICPMS) at the Institut de Physique du Globe de Paris, France. The operating and measurement conditions of this instrument are summarised in Table 3. For the isotope measurements, the samples were dissolved in 0.5 M HCl and introduced into the mass spectrometer using an ESI Apex-HF desolvator with a 100 μL min^{-1} PFA nebuliser. The Neptune was run in low resolution mode, with a mass resolution of ~1700 (M/ΔM as defined by the peak edge width from 5% to 95% full peak height; Table 3). The Pd isotopic composition of the sample and standard solutions were typically analysed at concentrations of 100 ppb Pd (i.e., samples were prepared with nominal Pd concentrations of 100 ng mL^{-1}, although in some cases samples were run at concentrations of ca. 50 ng mL^{-1}, against intensity matched standards). During Pd isotope measurements, ion beams at ^{102}Pd, ^{103}Rh, ^{104}Pd, ^{105}Pd, ^{106}Pd, ^{107}Ag, ^{108}Pd, ^{109}Ag, and ^{110}Pd were simultaneously collected in a single cycle using Faraday cups connected to amplifiers with $10^{11}\Omega$ resistors for all Pd channels. This configuration resulted in a combined ion beam intensity for all Pd isotopes of ~90 V at an uptake rate of ~100 μL min^{-1}, corresponding to a sensitivity of ~900 V ppm^{-1}. During some analytical tests, a second cycle was added in which ^{102}Pd was placed in the centre cup, permitting ^{98}Ru, ^{99}Ru, ^{100}Ru and ^{101}Ru to be collected in the low-mass side. Faraday collector gains were calibrated prior to the beginning of each analytical session.

Isotope results are reported in δ^{106}Pd notation, which reports the per mil (‰) difference in the ^{106}Pd/^{105}Pd ratio relative to our in-house Pd isotope standard (Pd_IPGP). All data reduction was conducted offline using the freely available double-spike data reduction tool *IsoSpike*(www.isospike.org; Creech and Paul, 2015).

4. RESULTS

4.1. Double-spike calibration

For precise determination of isotope ratios by double-spike, it is critical that the isotopic composition of the double-spike be accurately calibrated to the composition of the isotope standard. To correct for instrumental mass bias during the calibration we used external normalisation to a Ag ICP-standard solution, assuming natural abundances for the Ag isotopes (51.84% for ^{107}Ag and 48.16% for ^{109}Ag) from Meija et al. (2016). Measurements of both the reference standard and the double-spike solution had matched Ag:Pd concentrations (1:2) and instrumental mass

Table 3
Instrumental operating conditions and measurement parameter for the Neptune Plus MC-ICPMS.

Instrument operating conditions		
RF power		1300 W
Plasma cool gas flow rate		16 L min^{-1}
Interface cones	-sampler	Jet cone
	-skimmer	Ni skimmer, H-type
Source slit width		0.25 mm
Acceleration voltage		10 kV
Instrument resolution		~1700
Mass analyser pressure		ca. 8×10^{-9} mbar
Detector		9 Faraday detectors; all Pd channels using 10^{11} Ω preamplifiers
Sample introduction system		ESI Apex HF
Sample uptake rate		50 or 100 μL min^{-1}
Measurement parameters		
Solution concentration		100 ng;mL^{-1}
Typical sensitivity		~900 V;ppm^{-1} total Pd
Sample measurement time		100 × 8.4 s integrations
Washout time		~20 min
Background measurement time		100 × 8.4 s integrations, on-peak

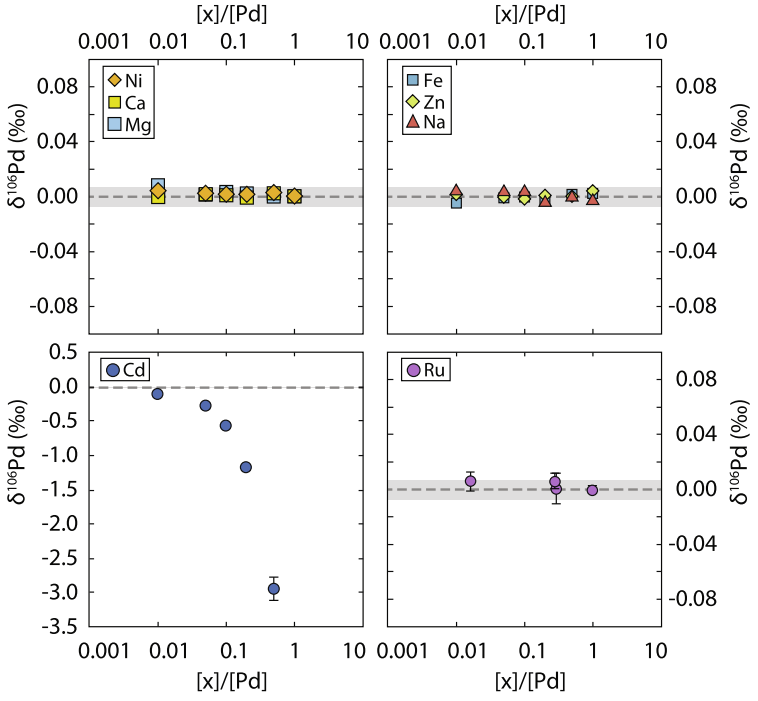

Fig. 4. Results of doping the Pd_IPGP standard at a range concentrations relative to Pd with various elements that are abundant in rocks (Na, Mg, Ca, Ni, Fe, Zn) or with potential for isobaric interferences in the mass range of Pd (Ru, Cd).

fractionation was corrected assuming an exponential fractionation law. In this approach with both the standard and double-spike measured in the same session, the calibration of the double-spike is relative to the calibration of the standard, and thus this method gives accurate results even if the absolute isotopic composition of Pd_IPGP is not precisely known. Ten analyses of both solutions were measured in the same session and the averages of these analyses assumed as the isotope ratios of each solution relative to each other.

The double-spike calibration was tested by analysing a series of double-spike–standard mixtures in different mixing proportions, with the proportion of double-spike varying from 0.2 to 0.7 (i.e., standard–spike ratio 4.0–0.4, or a factor of 0.38–1.3 times the theoretical optimal spike–sample proportion of 0.525). The results of these tests show that

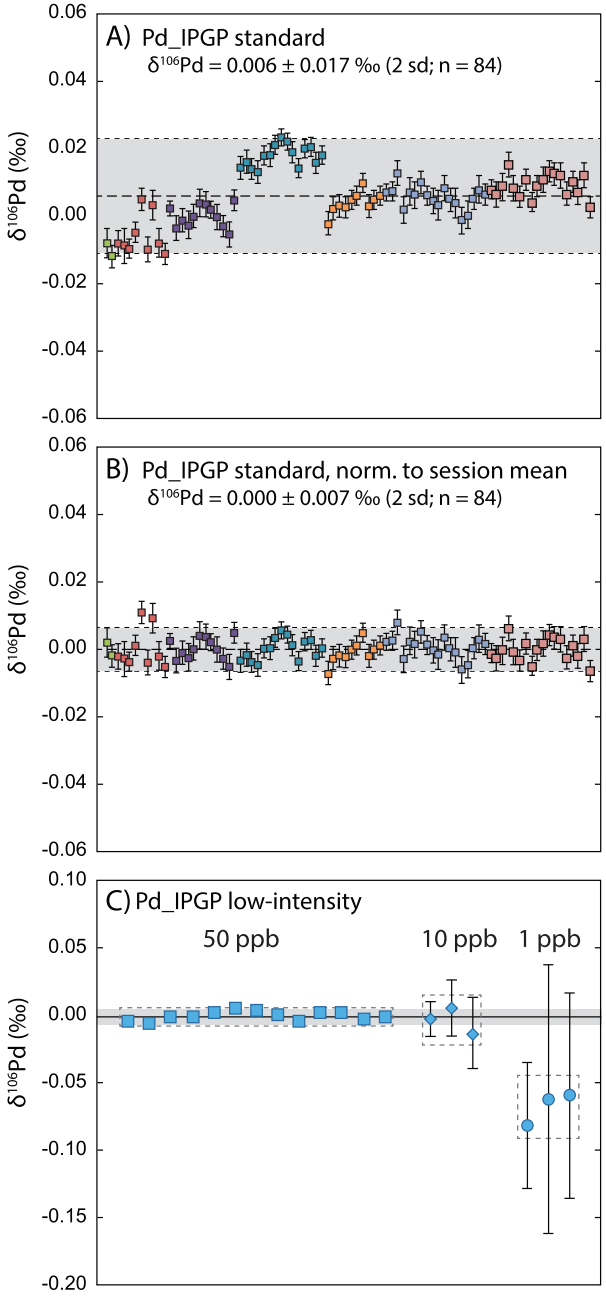

Fig. 5. (A) Pooled measurements of the Pd_IPGP standard over a period of ca. six months, with different coloured symbols corresponding to separate measurement sessions. Small offsets occur between measurement sessions, resulting in an external reproducibility of $\delta^{106}Pd = 0.006 \pm 0.017‰$ (2sd). (B) The same measurements of Pd_IPGP as in panel A, where data for each session has been renormalised such the session mean for Pd_IPGP has $\delta^{106}Pd = 0$, giving an external reproducibility of $\delta^{106}Pd = 0.000 \pm 0.007‰$ (2sd). (C) Results of analyses of Pd_IPGP standard at lower solution concentrations (as indicated) and thus lower signal intensities. Dashed boxes indicate the 2 sd uncertainty of the analyses they enclose. In all panels, error bars reflect the 2 se error of each analysis; where no error bars are visible, internal errors are smaller than the size of the data point.

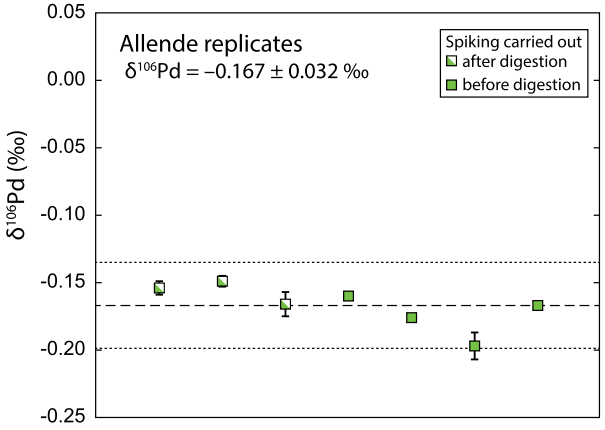

Fig. 6. Assessment of external reproducibility for natural samples based on seven replicate digestions of the carbonaceous chondrite Allende, which yield $\delta^{106}Pd = -0.167 \pm 0.032‰$.

the double-spike corrected values yield delta values ($\delta^{106}Pd$) that are within the typical reproducibility of measurements of the standard over this range of sample-spike mixtures (Fig. 2B). These results demonstrate that our double-spike approach should yield accurate results even when sample Pd concentrations are not well known at the time of double-spiking.

4.2. Isotopic fractionation associated with matrix effects

Non-spectral matrix effects may arise due to the presence of other elements besides the analyte in the sample solution, which may depress the ionisation and throughput of the analyte in the plasma. In order to test for such effects, solutions of the Pd_IPGP standard were doped with different elements (Na, Mg, Ca, Ni, Fe, Zn) in varying concentrations relative to Pd ([X]/[Pd] = 0.01–1.00; Fig. 4). These tests show that, using the double-spike approach, the presence of common rock-forming elements at proportions up to [X]/[Pd] = 1 do not impact our double-spike corrected results at levels comparable to our analytical reproducibility.

Due to the high relative abundances of ^{102}Ru and ^{104}Ru (31.6% and 18.7%, respectively), Pd isotope analyses at these masses may be strongly affected by the presence of Ru in samples. As described in Section 2.1 above, the choice of the ^{106}Pd–^{110}Pd was partly motivated by the avoidance of these interferences, and does not use ^{102}Pd or ^{104}Pd in the double-spike inversion. To confirm that the presence of Ru in our samples does not impact the double-spike corrected Pd isotope analyses, measurements of the Pd_IPGP standard were made with varying amounts of Ru (Fig. 4). At [Ru]/[Pd] up to ~1, double-spike corrected data remain within error of zero. Given that the relative yields of Pd and Ru from the chemical separation procedure are 96% and 37%, respectively, and that Pd and Ru are usually present in similar abundance in natural rocks, this demonstrates that our choice of double-spike inversion renders this approach insensitive to the presence of Ru at the levels that it is expected to be present in our samples.

Table 4
Pd stable isotope and concentration results for chondrites, ureilites and terrestrial samples from double-spike MC-ICPMS.

Sample	Total digested (g)	spiked before digestion?	δ^{106}Pd	±	*n*	Total Pd in sample (μg)	Pd conc. (μg g^{-1})	Ref. conc. (μg g^{-1})	meas./Ref. conc.	δ^{198}Pt	±
Chondrites											
Allende (CV3) replicates											
#1 (June 2015)	1.01	n	−0.154	0.005	1	547	542		0.77		
#2 (June 2015)	1.03	n	−0.149	0.004	1	542	526		0.75		
#3 (March 2016)	0.9939	n	−0.166	0.009	2	428	431		0.61		
#4 (March 2016)	0.7536	y	−0.160	0.003	2	529	702		1.00		
#5 (March 2016)	0.9035	y	−0.176	0.001	2	624	691		0.98		
#6 (Sept. 2016)	0.8470	y	−0.197	0.010	3	540	638		0.90		
#7 (Sept. 2016)	0.7072	y	−0.167	0.003	3	497	702		1.00		
Allende average			−0.167	0.032			605	705			
EET92002 (CK5)	0.614	y	−0.189	0.008	3	412	670				
Jbilet Winselwan (CM)	0.504	y	−0.239	0.010	3	303	602				
LON94101 (CM)	0.694	y	−0.220	0.003	3	424	611				
MIL090010 (CO)	0.921	y	−0.204	0.008	3	619	672				
BUC10933 (CR)	0.407	y	−0.197	0.008	3	284	697				
ALHA83010 (LL3.3)	0.454	y	−0.163	0.008	3	189	416				
MAC87302 (L4)	0.514	y	−0.155	0.007	3	291	567				
QUE97030 (H3.4)	0.520	y	−0.182	0.011	3	377	725				
Frenchmans Bay (H3.5)	0.446	y	−0.190	0.003	3	314	703				
SAH 97072 (EH3)	1.0281	y	−0.205	0.006	1	978	951				
Chondrite average			−0.192	0.050							
Ureilites											
ALHA77257	4.544	n	−0.184	0.004	1	72	15.9	27.4	0.58	−0.01	0.03
ALHA78019	0.274	n	−0.220	0.005	1	29	105.3	165.0	0.64	−0.21	0.04
ALHA81101	1.228	n	−0.201	0.006	1	47	37.9	33.0	1.15	0.17	0.13
ALHA84136	1.202	n	−0.220	0.004	1	91	75.6	78.3	0.97	−0.05	0.06
EET87157	1.091	n	−0.127	0.003	1	104	95.0	128.0	0.74	−0.05	0.06
EET96042	1.473	n	−0.225	0.003	1	135	91.9	112.0	0.82	−0.04	0.06
GRA95205	0.998	n	−0.237	0.004	1	59	58.9	84.3	0.70	−0.15	0.09
GRO95575	1.455	n	−0.167	0.006	1	63	43.3	21.6	2.00	0.10	0.14
META78008	0.741	n	−0.193	0.005	1	75	101.3	118.0	0.86	−0.11	0.07
PCA82506	1.778	n	−0.201	0.003	1	59	33.3	55.3	0.60	−0.19	0.02
Ureilite average			−0.197	0.065							
Terrestrial											
post-equilibration with late-veneer											
BC7 (peridotite; Nth. Qld, Australia)	12.7997	y	−0.228	0.009	3	44	3.5			−0.05	0.03
OKUM (komatiite; Abitibi Greenstone Belt, Canada; 2.7 Ga)	15.4272	y	−0.210	0.005	3	204	13.2	11.8	1.12	−0.17	0.08
LK-NIP (dolerite; Ontario, Canada)	18.3008	y	−0.108	0.004	3	357	19.5	18.0	1.09	−0.22	0.03

(*continued on next page*)

Table 4 (*continued*)

Sample	Total digested (g)	spiked before digestion?	δ^{106}Pd	±	*n*	Total Pd in sample (μg)	Pd conc. (μg g^{-1})	Ref. conc. (μg g^{-1})	meas./Ref. conc.	δ^{198}Pt	±
pre-equilibration with late-veneer											
B25 (komatiite; Barberton greenstone belt, 3.5 Ga)	9.9357	y	−0.134	0.008	1	30	3.0				
Isua supracrustal belt (3.8 Ga)											
460218 (metabasalt)	25.065	n	−0.258	0.004	1	123	4.9			0.09	0.05
460219 (metabasalt)	25.223	n	−0.123	0.004	1	69	2.7			0.13	0.07
460258 (metabasalt)	25.164	n	−0.311	0.003	1	119	4.7			−0.02	0.17
460275 (metabasalt)	20.396	n	−0.098	0.006	1	67	3.3				
duplicate	20.396	n	−0.223	0.007	1	59	2.9				
duplicate	14.9688	n	−0.251	0.006	1	101	6.7				
average			−0.191	0.162						0.11	0.05

Uncertainties on single measurements are the 2 se internal error for that analysis; where $n > 1$, data represent the mean and 2 sd of the analyses. The terrestrial samples are grouped according to whether they are inferred to represent compositions pre- or post-equilibration of the mantle with the late-veneer, as described in the text. Allende reference Pd concentration is the mean Allende value from Tagle and Berlin (2008), ureilite Pd concentrations are from Rankenburg et al. (2008), OKUM Pd concentration is from Wang and Becker (2014), and LK-NIP Pd concentration is the certificate value for that reference material. Pt data are from Creech et al. (2017).

Due to the possibility of isobaric interferences from Cd at masses 106, 108 and 110, we also made measurements of the Pd_IPGP standard doped with varying amounts of Cd (Fig. 4). Unsurprisingly, these tests showed that with our choice of double-spike inversion isotopes, double-spike corrected isotope ratios are significantly affected by the presence of small amounts of Cd. In our tests, even at the lowest [Cd]/[Pd] ratio (0.01), the Pd standard falls well outside the reproducibility of the method, and at higher amounts of Cd, isotope ratios tend towards extremely inaccurate values. These results indicate that double-spike corrected ratios will be affected at levels greater than our analytical reproducibility above [Cd]/[Pd] = 0.003. However, Cd is throughly separated from Pd during our sample digestion and chemistry, and in our natural samples, [Cd]/[Pd] ratios in Pd cuts were always 1–2 orders of magnitude lower than this threshold. Thus, Cd in natural samples is not considered to have had any effect on the accuracy of our double-spike corrected data.

4.3. Accuracy and reproducibility of double spike MC-ICP-MS measurements

4.3.1. Solution standards

Double-spike corrected analyses of the Pd_IPGP standard, under the analytical conditions given in Table 3, yield an internal precision on δ^{106}Pd of ca. 0.003‰ (2 se, $n = 100$). Within an analytical session, the 2 sd uncertainty of repeat measurements was typically on the order of ~0.007‰. However, offsets are observed between the Pd_IPGP averages from analytical sessions, which has a negative impact on the long-term apparent reproducibility, giving a mean of $\delta^{106}\text{Pd} = 0.006 \pm 0.017$‰ (2 sd, $n = 84$; Fig. 5A) over a period of ca. six months. Such offsets are often noted in double-spike studies (e.g., Schoenberg et al., 2008; Moeller et al., 2012; Creech et al., 2014), and may be related to small changes in the abundance sensitivity of the MC-ICPMS, drifts in the relative gains of the Faraday collectors, or a variable component of non-exponential mass bias that is not readily corrected for by the DS method. Therefore, the Pd compositions of unknowns are corrected for this offset by normalising to the session mean of Pd_IPGP measurements, which gives the long-term reproducibility on Pd_IPGP measurements of $\delta^{106}\text{Pd} = 0.000 \pm 0.007$‰ (2 sd, $n = 84$; Fig. 5B).

Analyses of Pd_IPGP were also made at lower signal intensities, with concentrations of 50 ng mL^{-1}, 10 ng mL^{-1} and 1 ng mL^{-1}, corresponding to ca. 40 ng, 8 ng and 0.8 ng of Pd consumed per analysis, respectively, as compared with ca. 80 ng for typical 100 ng/mL run solution. The results of this test are given in Fig. 5(C). Solutions with 50 ng mL^{-1} of Pd yield an average $\delta^{106}\text{Pd} = 0.00 \pm 0.01$‰, which is only marginally worse than those at 100 ng mL^{-1}. At 10 ng mL^{-1}, the average $\delta^{106}\text{Pd} = 0.00 \pm 0.02$‰, and at 1 ng mL^{-1} the data become inaccurate, giving $\delta^{106}\text{Pd} = -0.07 \pm 0.03$‰. Note that samples were typically run at a concentration of 100 ng mL^{-1}.

4.3.2. Natural samples

The reproducibility of our technique for samples with a geological matrix was tested by analysis of replicate digestions, ~0.7–1.0 g each, of the carbonaceous chondrite Allende taken from a homogenised powder prepared from a large (15 g) fragment of that meteorite (Fig. 6; Table 4). Of the seven replicate Allende samples, three were processed without double-spiking prior to digestion and four were double-spiked prior to digestion. While there is a small offset (ca. 0.020‰) between the means of samples spiked before and after chemistry, almost all analyses are within the 95% confidence interval of the mean of both groups, suggesting that there is no significant difference in samples spiked before or after digestion. However, a difference is apparent in the Pd concentration derived from these groups, indicating that the Pd recovery from the NiS fire assay method is variable and potentially as low as ca. 60%. The Pd concentrations derived from replicates that were spiked prior to NiS fire assay are consistent with literature data for Allende (average Pd ~705 ng/g; Tagle and Berlin, 2008). These data suggest that there is no significant isotopic fractionation arising from incomplete Pd yields from the NiS fire assay. Together, these replicates yield a mean Allende composition $\delta^{106}Pd = -0.167 \pm 0.032‰$ (2 sd). This is taken to represent the external reproducibility of the technique for natural samples, and error bars on subsequent plots of $\delta^{106}Pd$ are either the 2 sd uncertainty for that sample or the reproducibility based on Allende replicates, whichever is larger.

4.4. Natural Pd isotope variations

All data for natural samples are summarised in Table 4 and Fig. 7.

Data for 11 chondrites (six carbonaceous chondrites: 2 CM, 1 CV, 1 CO, 1 CR, 1 CK; four ordinary chondrites: 1 L, 1 LL, 2 H; one enstatite: 1 EH3), define a mean $\delta^{106}Pd = -0.19 \pm 0.05‰$, which is indistinguishable from the composition defined by replicates of Allende (Table 4; Fig. 7). The terrestrial samples analysed here define a terrestrial composition of $\delta^{106}Pd = -0.18 \pm 0.13‰$ (Table 4), although this terrestrial composition is discussed further in Section 5.2, below. On average, the ureilites have a Pd isotopic composition similar to that of chondrites, with a mean $\delta^{106}Pd = -0.197 \pm 0.065‰$ (2 sd). One ureilite sample, EET87157, appears to be an outlier, falling more than 2 sd from the mean. Excluding that sample from the mean gives $\delta^{106}Pd = -0.205 \pm 0.044‰$ (2 sd).

5. DISCUSSION

5.1. Palladium isotopic compositions of meteorites

The mean of 11 chondrites from all chondrite groups is indistinguishable from the composition defined by replicates of Allende (Table 4; Fig. 7), thus defining our chondritic Pd isotope composition, $\delta^{106}Pd_{chondrite} = -0.19 \pm 0.05‰$.

There is some indication of potential systematic variations between the different chondrite groups. With the exception of Allende and EET 92002 (CK5), all of the carbonaceous chondrites are isotopically lighter than the mean chondrite value. The single enstatite chondrite sample is also slightly isotopically lighter than the mean, similar to the carbonaceous chondrites. Amongst the ordinary chondrites, the H chondrites are very close to the mean value, whereas the L chondrites are the isotopically heaviest chondrite samples. However, these variations are not significant relative to our analytical uncertainties, and further analyses are required to confirm this speculation.

The largest compositional range is observed amongst the carbonaceous chondrites, which could potentially indicate the presence of uncorrected mass-independent effects in those samples arising from the greater proportions of matrix and refractory inclusions (amoeboid olivine aggregates and Ca–Al-rich inclusions) found in that group, similar to observations made for Pt stable isotopes (Creech et al., 2017). Given that $\delta^{106}Pd$ represents a mass difference

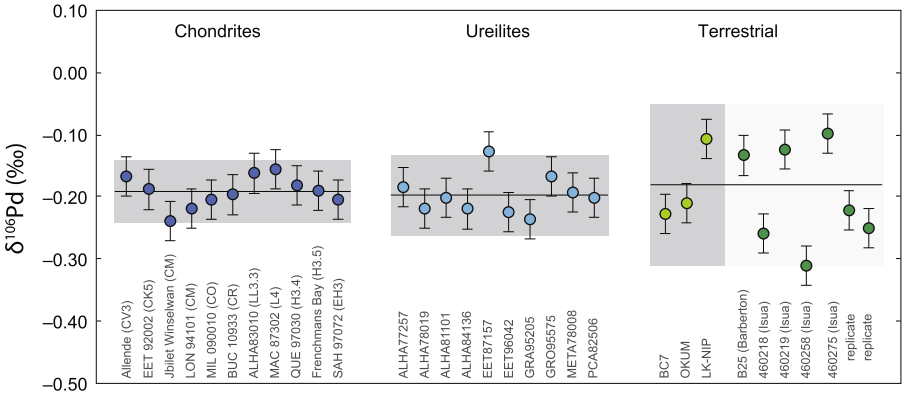

Fig. 7. $\delta^{106}Pd$ data for chondrite and ureilite meteorites and terrestrial samples. Error bars represent the 2 sd uncertainty for each sample or the reproducibility of the technique based on replicate measurements of Allende (i.e., ±0.032‰), whichever is larger. Shaded boxes and horizontal lines represent the mean and 2 sd of the samples they enclose. The terrestrial samples are separated as described in the text, with the present-day mantle composition being defined by the three youngest samples. The terrestrial composition is extended over the Archean samples, which are all within uncertainty of $\delta^{106}Pd_{mantle}$.

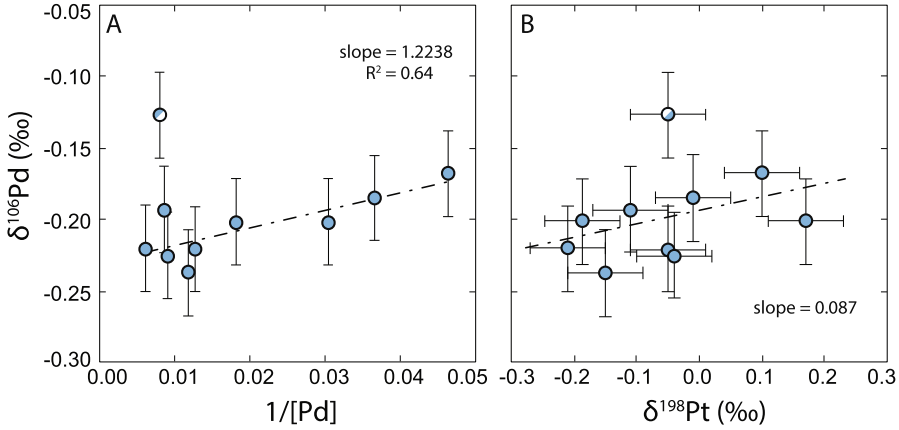

Fig. 8. (A) Ureilite δ^{106}Pd data vs. 1/[Pd], where [Pd] is the Pd concentration in ng g^{-1}. Note that the Pd concentrations from Rankenburg et al. (2008) were used in lieu of our concentrations as double-spiking was not carried out before digestion for these samples. (B) Ureilite δ^{106}Pd data vs. δ^{198}Pt. Note that a 1:1 correlation with Pt isotope data would yield a slope of ~0.25, as δ^{198}Pt represents a mass difference of 4 amu, compared with 1 amu for δ^{106}Pd. Note that in both panels, the regression through the data excludes the sample EET87157, indicated by the half filled symbol, as an outlier, as it falls outside of a 2 sd error envelope.

of only 1 amu, the compositional range observed in chondrites is significant, and further investigations of these components are warranted. However, the mean of seven replicate digestions from a large homogenised sample of Allende is indistinguishable to that of all ordinary and enstatite chondrites, indicating that the bulk value of all chondrite groups is identical within our uncertainties.

The suite of ureilites presented here was also analysed for Pt stable isotopes by Creech et al. (2017) and showed range of Pt isotope compositions with a correlation between δ^{198}Pt and Pt concentration, which was interpreted to reflect Pt stable isotopic fractionation during metal–silicate partitioning. The range observed in Pd stable isotope compositions of ureilites is significantly smaller than that for Pt (Table 4; Fig. 7), indicating that Pd isotopes are less strongly fractionated during metal–silicate differentiation. A subtle correlation is observed between Pd stable isotope compositions and Pd concentrations in ureilites, and a regression through δ^{106}Pd vs 1/[Pd] gives a slope of 1.2 with an $R^2 = 0.64$ (Fig. 8A). This slope suggests a Pd isotopic of fractionation 0.3 ppm per ng g^{-1} of Pd depletion. However, given the small range in Pd isotope compositions relative to our uncertainties, this correlation does not give a strong indication that a measurable Pd isotopic fractionation would be expected to accompany metal–silicate planetary differentiation. The Pd stable isotope data show a moderate correlation with Pt stable isotopes, where a linear regression through δ^{106}Pd vs. δ^{198}Pt gives a slope of 0.087 (Fig. 8); note that a 1:1 correlation would have a slope of 0.25, as δ^{198}Pt represents a mass difference of four amu, compared with one amu for δ^{106}Pd. The smaller range in Pd stable isotopes and weaker correlation with Pd concentration as compared with Pt may relate to the weaker partitioning of Pd between metal and silicate ($D_{Pd}^{met/sil} \sim 10^3$–$10^4$ vs. $D_{Pt}^{met/sil} \sim 10^4$–$10^5$), or may support the idea that nuclear volume effects play a more significant role in stable isotope fractionation for the heavier element Pt as compared with Pd, as has been observed for other elements (Schauble, 2007; Fujii et al., 2009; Moynier et al., 2013).

5.2. Palladium isotopic composition of Earth's mantle

The terrestrial samples we analysed represent different compositions, geological settings and ages. These samples also span a range of Pd stable isotopic compositions that exceeds that observed in the meteorite samples analysed so far.

In Pt stable isotope data (Creech et al., 2017), Archean samples from Isua have been recently shown to have heavy, non-chondritic Pt stable isotope compositions, potentially indicating preservation of some fraction of a pre-late-veneer signature of core-formation (Creech et al., 2017). As such, we draw a distinction between some Archean samples in this study, as these may pre-date the complete equilibration of late-veneer with the upper mantle. Maier et al. (2009) showed, based on komatiite data, that PGE contents of the mantle increased through the Archean (4.5–2.9 Ga), which has been interpreted to reflect the progressive equilibration of late-veneer material with the mantle. Thus, the ~3.8 Ga Isua suite and the ~3.5 Ga komatiite B25 are treated as a separate group. The komatiite sample OKUM, while Archean, has an age of ~2.7 Ga, and it thus considered to represent mantle that had fully equilibrated with the late-veneer. Furthermore, OKUM has been shown to have a Pt stable isotope composition that is identical to the modern, chondritic mantle (Creech et al., 2014, 2017). The mantle-derived samples BC7 and OKUM may best characterise the upper mantle, suggesting a $\delta^{106}Pd_{mantle} = -0.22 \pm 0.03‰$. However, there is no evidence yet that igneous processes fractionate Pd stable isotopes, and given that the dolerite sample LK-NIP also has a mantle-like Pt stable isotope composition (Creech et al., 2014), it cannot be readily excluded. Thus, we derive a terrestrial mantle value $\delta^{106}Pd_{mantle} = -0.18 \pm 0.13‰$. Further analyses of

terrestrial samples may refine this value. Based on our data so far, the mantle Pd isotope composition is indistinguishable from that of chondrites. At present is not clear that core formation would have imparted a Pd isotopic signature on Earth's mantle, and thus we cannot say conclusively that a chondritic Pd isotopic composition in the mantle requires a chondritic late-veneer. However, a chondritic isotopic signature remains fully consistent with that hypothesis.

Archean samples from Isua have been recently shown to have heavy, non-chondritic Pt stable isotope compositions, potentially indicating preservation of some fraction of a pre-late-veneer signature of core-formation (Creech et al., 2017). Conversely, Pd stable isotopes in the same samples are within error of our current estimate of the modern mantle composition (Fig. 7). The lack of a heavy isotopic signature could indicate either that Pd isotopes were not fractionated to the same extent as Pt during core formation, or that the Pd has been impacted by secondary processes occurring in the crust. The Isua supracrustals have been variably affected by metamorphism, as indicated by disturbances in their Sm-Nd and Lu-Hf systematics (e.g., Rizo et al., 2011, 2013). In detail, three of the four Isua samples analysed in this study show uncorrelated ϵ^{143}Nd(T) (calculated at 3.8 Gyr) and μ^{142}Nd variations indicative of disturbance of the Sm-Nd systematics (Rizo et al., 2013). Despite this, Pt stable isotope data show virtually no variability beyond the analytical uncertainties for the same samples ($\delta^{198}\text{Pt} = +0.09 \pm 0.07‰$; 2sd; Creech et al., 2017), while the Pd isotopes show significant variability (Fig. 7). The variability in the Pd stable isotope data could indicate that Pd is less robust than Pt during secondary processes.

6. CONCLUSIONS

The new method presented in this paper allows for near quantitative extraction of Pd from geological samples suitable for high-precision isotope ratios measurements by double-spike MC-ICPMS. Using this new technique the first important results are as follows.

- Replicate digestions of the carbonaceous chondrite Allende demonstrate the external reproducibility of the technique of ±0.032‰ on δ^{106}Pd.
- Chondrites define a mean $\delta^{106}\text{Pd}_{\text{chondrite}} = -0.19 \pm 0.05‰$.
- Ureilites data suggest that Pd isotopes are significantly less fractionated during metal–silicate segregation than for Pt, likely due to its weaker metal–silicate partitioning behaviour or the lesser impact of nuclear volume effects at the mass of Pd.
- Terrestrial mantle samples analysed so far give a $\delta^{106}\text{Pd}_{\text{mantle}} = -0.18 \pm 0.13‰$, which is consistent with a late-veneer of chondritic material after core formation.

Our data show that the Pd stable isotope system holds considerable potential for studying a range of geological and planetary processes.

ACKNOWLEDGEMENTS

The authors wish to thank Michael Storey for providing the Isua samples, NASA-JSC/Joel Baker for providing ureilite samples, and Monica Handler for the sample BC7. We also thank Jennifer Benchetrit for performing some laboratory work during a summer internship. We also gratefully acknowledge three anonymous reviewers for their detailed and constructive comments on the manuscript, and Marc-Alban Millet for his efficient editorial handling. F.M. acknowledges funding from the European Research Council [ERC Starting grant agreement 637503-Pristine] to as well as the financial support of the UnivEarthS Labex program at Sorbonne Paris Cité [ANR-10-LABX-0023 and ANR-11-IDEX-0005-02] and a chaire d' excellence ANR-Idex Sorbonne Paris Cité. Parts of this work were supported by the IPGP multidisciplinary PARI program and Region Île-de-France SESAME Grant No. 12015908. MB acknowledges support from European Research Council [ERC Consolidator grant agreement 616027-STARDUST2ASTEROIDS] and the Danish National Research Foundation [grant #DNRF97].

REFERENCES

Abraham K., Barling J., Siebert C., Belshaw N., Gall L. and Halliday A. N. (2015) Determination of mass-dependent variations in tungsten stable isotope compositions of geological reference materials by double-spike and MC-ICPMS. *J. Anal. At. Spectrom.* **30**(11), 2334–2342.

Anbar A. D., Knab K. A. and Barling J. (2001) Precise determination of mass-dependent variations in the isotopic composition of molybdenum using MC-ICPMS. *Anal. Chem.* **73**(7), 1425–1431.

Arnold T., Schönbächler M., Rehkämper M., Dong S., Zhao F.-J., Kirk G. J. D., Coles B. J. and Weiss D. J. (2010) Measurement of zinc stable isotope ratios in biogeochemical matrices by double-spike MC-ICPMS and determination of the isotope ratio pool available for plants from soil. *Anal. Bioanal. Chem.* **398**(7–8), 3115–3125.

Baadsgaard H., Nutman A. P., Bridgwater D., Rosing M., McGregor V. R. and Allaart J. H. (1984) The zircon geochronology of the Akilia association and Isua supracrustal belt, West Greenland. *Earth Planet. Sci. Lett.* **68**(2), 221–228.

Baker J., Peate D., Waight T. and Meyzen C. (2004) Pb isotopic analysis of standards and samples using a ^{207}Pb-^{204}Pb double spike and thallium to correct for mass bias with a double-focusing MC-ICP-MS. *Chem. Geol.* **211**(3–4), 275–303.

Barrat J. A., Rouxel O., Wang K., Moynier F., Yamaguchi A., Bischoff A. and Langlade J. (2015) Early stages of core segregation recorded by Fe isotopes in an asteroidal mantle. *Earth Planet. Sci. Lett.* **419**, 93–100.

Beard B. L. and Johnson C. M. (1999) High precision iron isotope measurements of terrestrial and lunar materials. *Geochim. Cosmochim. Acta* **63**(11–12), 1653–1660.

Beard B. L., Johnson C. M., Cox L., Sun H., Nealson K. H. and Aguilar C. (1999) Iron isotope biosignatures. *Science* **285**(5435), 1889–1892.

Bezard R., Fischer-Gödde M., Hamelin C., Brennecka G. A. and Kleine T. (2016) The effects of magmatic processes and crustal recycling on the molybdenum stable isotopic composition of Mid-Ocean Ridge Basalts. *Earth Planet. Sci. Lett.* **453**, 171–181.

Bonnand P., Williams H. M., Parkinson I. J., Wood B. J. and Halliday A. N. (2016) Stable chromium isotopic composition of meteorites and metal–silicate experiments: Implications for

fractionation during core formation. *Earth Planet. Sci. Lett.* **435**, 14–21.

Borisov A., Palme H. and Spettel B. (1994) Solubility of palladium in silicate melts: implications for core formation in the Earth. *Geochim. Cosmochim. Acta* **58**(2), 705–716.

Burkhardt C., Hin R. C., Kleine T. and Bourdon B. (2014) Evidence for Mo isotope fractionation in the solar nebula and during planetary differentiation. *Earth Planet. Sci. Lett.* **391**, 201–211.

Caro G., Bourdon B., Birck J.-L. and Moorbath S. (2006) High-precision $^{142}Nd/^{144}Nd$ measurements in terrestrial rocks: constraints on the early differentiation of the Earth's mantle. *Geochim. Cosmochim. Acta* **70**(1), 164–191.

Compston W. and Oversby V. M. (1969) Lead isotopic analysis using a double spike. *J. Geophys. Res.* **74**(17), 4338–4348.

Creech J., Baker J., Handler M., Schiller M. and Bizzarro M. (2013) Platinum stable isotope ratio measurements by double-spike multiple collector ICPMS. *J. Anal. At. Spectrom.* **28**, 853–865.

Creech J., Baker J., Handler M. and Bizzarro M. (2014) Platinum stable isotope analysis of geological standard reference materials by double-spike MC-ICPMS. *Chem. Geol.* **363**, 293–300.

Creech J., Baker J., Handler M., Lorand J.-P., Storey M., Wainwright A., Luguet A., Moynier F. and Bizzarro M. (2017) Late accretion history of the terrestrial planets inferred from platinum stable isotopes. *Geochem. Perspect. Lett.*, 94–104.

Creech J. and Paul B. (2015) *IsoSpike*: improved double-spike deconvolution software. *Geostand. Geoanal. Res.* **39**, 7–15.

Dennen W. H. (1954) *Some Aspects of the Geochemistry of Platinum, Palladium, and Gold in Igneous Rocks with Special Reference to the Bushveld Complex, Transvaal* (Ph.D). Massachusetts Institute of Technology.

Dideriksen K., Baker J. and Stipp S. (2006) Iron isotopes in natural carbonate minerals determined by MC-ICP-MS with a ^{58}Fe-^{54}Fe double spike. *Geochim. Cosmochim. Acta* **70**(1), 118–132.

Elardo S. M. and Shahar A. (2017) Non-chondritic iron isotope ratios in planetary mantles as a result of core formation. *Nat. Geosci.*, advance online publication.

Eugster O., Tera F. and Wasserburg G. J. (1969) Isotopic analyses of barium in meteorites and in terrestrial samples. *J. Geophys. Res.* **74**(15), 3897–3908.

Fujii T., Moynier F. and Albarède F. (2009) The nuclear field shift effect in chemical exchange reactions. *Chem. Geol.* **267**(3–4), 139–156.

Fujii T., Moynier F., Agranier A., Ponzevera E. and Abe M. (2011) Isotope fractionation of palladium in chemical exchange reaction. *Proc. Radiochem. A Suppl. Radiochim. Acta* **1**(1), 339–344.

Gall L., Williams H., Siebert C. and Halliday A. (2012) Determination of mass-dependent variations in nickel isotope compositions using double spiking and MC-ICPMS. *J. Anal. At. Spectrom.* **27**(1), 137.

Gopalan K., Macdougall D. and Macisaac C. (2006) Evaluation of a ^{42}Ca–^{43}Ca double-spike for high precision Ca isotope analysis. *Int. J. Mass Spectrom.* **248**(1–2), 9–16.

Greenwood, R.C., Burbine, T.H., Miller, M.F., Franchi, I.A., 2016. Melting and Differentiation of Early-formed Asteroids: The Perspective from High Precision Oxygen Isotope Studies. Chemie der Erde – Geochemistry.

Hamelin B., Manhes G., Albarede F. and Allègre C. J. (1985) Precise lead isotope measurements by the double spike technique: a reconsideration. *Geochim. Cosmochim. Acta* **49**(1), 173–182.

Hart T. R. and MacDonald C. A. (2007) Proterozoic and Archean geology of the Nipigon Embayment: implications for emplacement of the Mesoproterozoic Nipigon diabase sills and mafic to ultramafic intrusions. *Can. J. Earth Sci.* **44**(8), 1021–1040.

Heaman L., Easton R., Hart T., Hollings P., MacDonald C. and Smyk M. (2007) Further refinement to the timing of Mesoproterozoic magmatism, Lake Nipigon region, Ontario. *Can. J. Earth Sci.* **44**(8), 1055–1086.

Hin R. C., Burkhardt C., Schmidt M. W., Bourdon B. and Kleine T. (2013) Experimental evidence for Mo isotope fractionation between metal and silicate liquids. *Earth Planet. Sci. Lett.* **379**, 38–48.

Holzheid A., Sylvester P., O'Neill H. S., Rubie D. C. and Palme H. (2000) Evidence for a late chondritic veneer in the Earth's mantle from high-pressure partitioning of palladium and platinum. *Nature* **406**(6794), 396–399.

Hopp T., Fischer-Gödde M. and Kleine T. (2016) Ruthenium stable isotope measurements by double spike MC-ICPMS. *J. Anal. At. Spectrom.*.

Houlé M. G., Préfontaine S., Fowler A. D. and Gibson H. L. (2009) Endogenous growth in channelized komatiite lava flows: evidence from spinifex-textured sills at Pyke Hill and Serpentine Mountain, Western Abitibi Greenstone Belt, Northeastern Ontario, Canada. *Bull. Volcanol.* **71**(8), 881–901.

Kaye G. W. C. and Laby T. H. (1995) *Tables of Physical and Chemical Constants*, 16th ed. Kaye & Laby Online, London.

Krabbe N., Kruijer T. S. and Kleine T. (2017) Tungsten stable isotope compositions of terrestrial samples and meteorites determined by double spike MC-ICPMS. *Chem. Geol.* **450**, 135–144.

Lodders K. (2003) Solar system abundances and condensation temperatures of the elements. *Astrophys. J.* **591**(2), 1220.

Mahan B., Siebert J., Pringle E. A. and Moynier F. (2017) Elemental partitioning and isotopic fractionation of Zn between metal and silicate and geochemical estimation of the S content of the Earth's core. *Geochim. Cosmochim. Acta* **196**, 252–270.

Maier W. D., Barnes S. J., Campbell I. H., Fiorentini M. L., Peltonen P., Barnes S. and Smithies R. H. (2009) Progressive mixing of meteoritic veneer into the early Earth's deep mantle. *Nature* **460**(7255), 620–623.

Mann U., Frost D. J., Rubie D. C., Becker H. and Audétat A. (2012) Partitioning of Ru, Rh, Pd, Re, Ir and Pt between liquid metal and silicate at high pressures and high temperatures – implications for the origin of highly siderophile element concentrations in the Earth's mantle. *Geochim. Cosmochim. Acta* **84**, 593–613.

Mayer B., Wittig N., Humayun M. and Leya I. (2015) Palladium isotopic evidence for nucleosynthetic and cosmogenic isotope anomalies in IVB iron meteorites. *Astrophys. J.* **809**(2), 180.

McDonough W. F. (2014) 3.16 – compositional model for the Earth's core. In *Treatise on Geochemistry* (ed. H. D. H. K. Turekian), second ed. Elsevier, Oxford, pp. 559–577.

Meija J., Coplen T. B., Berglund M., Brand W. A., De B. P., Gröning M., Holden N. E., Irrgeher J., Loss R. D., Walczyk T. and Prohaska T. (2016) Isotopic compositions of the elements 2013 (IUPAC Technical Report). *Pure Appl. Chem.* **88**(3), 293–306.

Michard-Vitrac A., Lancelot J., Allègre C. J. and Moorbath S. (1977) U-Pb ages on single zircons from the Early Precambrian rocks of West Greenland and the Minnesota River Valley. *Earth Planet. Sci. Lett.* **35**(3), 449–453.

Millet M.-A., Dauphas N., Greber N. D., Burton K. W., Dale C. W., Debret B., Macpherson C. G., Nowell G. M. and Williams H. M. (2016) Titanium stable isotope investigation of magmatic processes on the Earth and Moon. *Earth Planet. Sci. Lett.* **449**, 197–205.

Moeller K., Schoenberg R., Pedersen R.-B., Weiss D. and Dong S. (2012) Calibration of the new certified reference materials ERM-AE633 and ERM-AE647 for copper and IRMM-3702 for zinc isotope amount ratio determinations. *Geostand. Geoanal. Res.* **36**(2), 177–199.

Moynier F., Fujii T., Brennecka G. A. and Nielsen S. G. (2013) Nuclear field shift in natural environments. *C.R. Geosci.* **345**(3), 150–159.

Nanne, J.A.M., Millet, M.-A., Burton, K.W., Dale, C.W., Nowell, G., Williams, H.M., Mar. 2017. High Precision Osmium Stable Isotope Measurements by Double Spike MC-ICP-MS and N-TIMS.

Nutman A. P., Mojzsis S. J. and Friend C. R. L. (1997) Recognition of $\geqslant$3850 Ma water-lain sediments in West Greenland and their significance for the early Archaean Earth. *Geochim. Cosmochim. Acta* **61**(12), 2475–2484.

Rankenburg K., Humayun M., Brandon A. and Herrin J. (2008) Highly siderophile elements in ureilites. *Geochim. Cosmochim. Acta* **72**(18), 4642–4659.

Rizo H., Boyet M., Blichert-Toft J. and Rosing M. (2011) Combined Nd and Hf isotope evidence for deep-seated source of Isua lavas. *Earth Planet. Sci. Lett.* **312**(3–4), 267–279.

Rizo H., Boyet M., Blichert-Toft J. and Rosing M. T. (2013) Early mantle dynamics inferred from ^{142}Nd variations in Archean rocks from southwest Greenland. *Earth Planet. Sci. Lett.*, 324–335.

Rudge J. F., Reynolds B. C. and Bourdon B. (2009) The double spike toolbox. *Chem. Geol.* **265**(3–4), 420–431.

Schauble E. A. (2007) Role of nuclear volume in driving equilibrium stable isotope fractionation of mercury, thallium, and other very heavy elements. *Geochim. Cosmochim. Acta* **71**(9), 2170–2189.

Schoenberg R., Zink S., Staubwasser M. and von Blanckenburg F. (2008) The stable Cr isotope inventory of solid Earth reservoirs determined by double spike MC-ICP-MS. *Chem. Geol.* **249**(3–4), 294–306.

Scott E. R. D., Taylor G. J. and Keil K. (1993) Origin of ureilite meteorites and implications for planetary accretion. *Geophys. Res. Lett.* **20**(6), 415–418.

Siebert C., Nägler T. F. and Kramers J. D. (2001) Determination of molybdenum isotope fractionation by double-spike multicollector inductively coupled plasma mass spectrometry. *Geochem. Geophys. Geosyst.* **2**(7), 16.

Tagle R. and Berlin J. (2008) A database of chondrite analyses including platinum group elements, Ni, Co, Au, and Cr: implications for the identification of chondritic projectiles. *Meteorit. Planet. Sci.* **43**(3), 541–559.

Wang Z. and Becker H. (2014) Abundances of sulfur, selenium, tellurium, rhenium and platinum-group elements in eighteen reference materials by isotope dilution sector-field ICP-MS and Negative TIMS. *Geostand. Geoanal. Res.* **38**(2), 189–209.

Warren P. H., Ulff-Møller F., Huber H. and Kallemeyn G. W. (2006) Siderophile geochemistry of ureilites: a record of early stages of planetesimal core formation. *Geochim. Cosmochim. Acta* **70**(8), 2104–2126.

Young E. D., Manning C. E., Schauble E. A., Shahar A., Macris C. A., Lazar C. and Jordan M. (2015) High-temperature equilibrium isotope fractionation of non-traditional stable isotopes: experiments, theory, and applications. *Chem. Geol.* **395**, 176–195.

Associate editor: Marc-Alban Millet